






Syntheses, crystal structures, and electrochemistry of novel Fe₂SN and FeSN carbonyl complexes with pendant bases

Yao-Cheng Shi, Ying Shi, Jin-Ping Li, Qing Tan, Wei Yang & Sun Xie


To cite this article: Yao-Cheng Shi, Ying Shi, Jin-Ping Li, Qing Tan, Wei Yang & Sun Xie (2015) Syntheses, crystal structures, and electrochemistry of novel Fe₂SN and FeSN carbonyl complexes with pendant bases, Journal of Coordination Chemistry, 68:15, 2620-2632, DOI: [10.1080/00958972.2015.1062479](https://doi.org/10.1080/00958972.2015.1062479)


To link to this article: <http://dx.doi.org/10.1080/00958972.2015.1062479>

 View supplementary material 



 Accepted author version posted online: 15 Jun 2015.
Published online: 24 Jul 2015.

 Submit your article to this journal 

 Article views: 60

 View related articles 

 View Crossmark data 

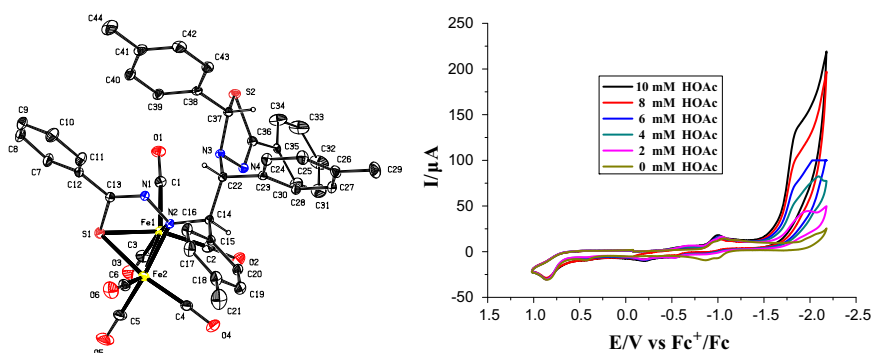
 Citing articles: 1 View citing articles 

Syntheses, crystal structures, and electrochemistry of novel Fe_2SN and FeSN carbonyl complexes with pendant bases

YAO-CHENG SHI*, YING SHI, JIN-PING LI, QING TAN, WEI YANG and SUN XIE

College of Chemistry and Chemical Engineering, Yangzhou University, Yangzhou, PR China

(Received 20 February 2015; accepted 6 May 2015)



Reactions of $\text{Fe}_2(\text{CO})_9$ with thioacylhydrazones $\text{ArCH}=\text{NNHCSPH}$ in THF afford $\text{Fe}_2(\text{CO})_6(\mu-\kappa^2\text{S}:\kappa^2\text{N}-\text{PhC}(\text{S})=\text{NNCHArCHARN}(\text{CHAR})\text{N}=\text{CSPH})$ (**1**, $\text{Ar}=\text{C}_6\text{H}_5$; **3**, $\text{Ar}=4\text{-CH}_3\text{C}_6\text{H}_4$) and $\text{Fe}(\text{CO})_3(\kappa^2\text{S}:\text{N}-\text{PhC}(\text{S})=\text{NNHCHArCHARN}(\text{CHAR})\text{N}=\text{CSPH})$ (**2**, $\text{Ar}=\text{C}_6\text{H}_5$; **4**, $\text{Ar}=4\text{-CH}_3\text{C}_6\text{H}_4$). They have been characterized by elemental analyses, IR, ^1H NMR, and ^{13}C NMR and structurally determined by X-ray crystallography. Electrochemical studies reveal that when using HOAc as a proton source, they exhibit high catalytic H_2 -production.

Keywords: Hydrogenase; Carbonyl iron; Thio-Schiff base; Cyclic voltammetry; H_2 evolution

1. Introduction

Hydrogenase enzymes, one of the rare families of organometallic biomolecules, very efficiently catalyze the reductive generation and oxidative uptake of molecular hydrogen. Consequently, simpler $[\text{Fe}_2\text{S}_2]$ catalysts based on these enzymes have been studied [1–6]. The goal was to develop cheap, robust, and reliable catalysts that produce dihydrogen to empower a future hydrogen energy economy. The enzymes typically feature binuclear active sites: either iron and nickel, $[\text{NiFe}]$ hydrogenases or two iron ions, $[\text{FeFe}]$ hydrogenases. The $[\text{FeFe}]$ hydrogenases contain an Fe_2S_2 core as their active sites and are especially well-suited for reductive hydrogen generation. Models based on the $[\text{NiFe}]$

*Corresponding author. Email: yeshi@yzu.edu.cn

hydrogenases have shown promise [7–9]. Catalysts based on the [FeFe] hydrogenases have progressed much further [10–15]. However, novel structural and chemical models are still necessary to gain a better understanding of the protonation mechanisms at the molecular level [2, 16]. Studies on modeling the diiron subsite of [FeFe] hydrogenases have led to a significant renaissance in the chemistry of sulfur-rich diiron carbonyls; in this context, we have recently initiated a project developing synthetic methodologies for Fe/S and Fe/Se cluster complexes for model compounds [17–23]. As part of the ongoing project, in this article we report the syntheses, crystal structures, and electrochemistry of Fe₂SN and FeSN carbonyl complexes with pendant bases.

2. Experimental

2.1. Materials and physical measurements

All reactions were carried out under N₂ with standard Schlenk techniques. All solvents employed were dried by refluxing over appropriate drying agents and stored under N₂ atmosphere. THF was distilled from sodium-benzophenone, petroleum ether (60–90 °C) and CH₂Cl₂ from P₂O₅. PhCSNHNH₂ and ArCH=NNHCSPH (Ar = C₆H₅ and 4-CH₃C₆H₄) [24–26] were prepared using modified methods. A solution of PhCSNHNH₂ (1.522 g, 10 mmol) and ArCHO (10 mmol for PhCHO, 1.061 g; 10 mmol for 4-CH₃C₆H₄CHO, 1.201 g) in 25 mL of EtOH was stirred for 12 h, ArCH=NNHCSPH was obtained as white solid in yields of 62 and 57%. The progress of all reactions was monitored by TLC. ¹H and ¹³C NMR measurements were carried out on a Bruker Avance 600 or an Agilent 400 spectrometer. IR spectra were recorded on a Bruker Tensor 27 spectrometer as KBr disks from 400 to 4000 cm⁻¹. Electrochemical measurements were made using a BAS Epsilon or CHI760D potentiostat. Analyses for C, H, and N were performed on an Elementar Vario EL analyzer. Melting points were measured on an X-6 apparatus and are uncorrected.

2.2. Syntheses of Fe₂(CO)₆(μ-κ²S:κ²N-PhC(S)=NNCHPhCHPhN(CHPh)N=CSPH) (1) and Fe(CO)₃(κ²S:N-PhC(=S)NHNCHPhCHPhN(CHPh)N=CSPH) (2)

A 100-mL Schlenk flask equipped with a stir bar and serum cap was charged with 0.728 g (2 mmol) of Fe₂(CO)₉, 0.240 g (1 mmol) of C₆H₅CH=NNHCSPH, and 25 mL of THF. The mixture was stirred for 24 h at room temperature and then filtered. After the solvent was removed under reduced pressure, the resulting residue was chromatographed using TLC on silica gel. Elution with petroleum ether gave one orange band and a brown-red band in decreasing order of R_f values. The first band afforded a red solid of **1** (0.128 g) in 30% yield. Mp., 120–122 °C. Anal. Calcd for C₄₁H₂₈Fe₂N₄O₆S₂ (**1**) (%): C 58.04; H, 3.33; N, 6.60; found: C, 58.29; H, 3.47; N, 6.52. IR (KBr disk): 3081 (w), 3060 (w), 3027 (m), 2955 (w), 2924 (m), 2074 (s), 2004 (vs), 1937 (s), 1983 (vs), 1596 (w), 1582 (w), 1552 (w), 1490 (w), 1451 (w), 1288 (w), 1255 (w), 1178 (w), 761 (m), 700 (m) cm⁻¹. ¹H NMR (600 MHz, CDCl₃, TMS): δ 6.86–7.59 (m, 25H, 5C₆H₅), 5.44 (s, 1H), 4.58, 4.32 (d, d, ³J = 12 Hz, 1H, 1H, CHCH). ¹³C NMR (125 MHz, CDCl₃, TMS): δ 214.5, 210.9, 209.4, 208.3, 203.2, 163.3, 147.1, 131.9, 130.6, 129.2, 129.0, 128.9, 128.8, 128.6, 128.3, 127.4, 127.2, 127.1, 126.7, 126.3, 84.3, 77.3, 69.1. The second band afforded a red solid of **2** (0.061 g) in 17% yield. Mp., 92–93 °C. Anal. Calcd for C₃₈H₂₉FeN₄O₃S₂ (**2**) (%): C 64.32;

H, 4.12; N, 7.90; found: C, 64.41; H, 4.09; N, 7.86. IR (KBr disk): 3348 (m), 3073 (w), 3034 (m), 2067 (s), 2041 (s), 1996 (vs), 1605 (vs), 1499 (vs), 1467 (w), 1275 (s), 1176 (m), 1025 (w), 994 (w), 960 (w), 880 (m), 818 (w), 753 (vs), 691 (s) cm^{-1} . ^1H NMR (400 MHz, CDCl_3 , TMS): δ 6.96–7.97 (m, 25H, $5\text{C}_6\text{H}_5$), 5.85 (s, 1H), 5.76 (s, 1H), 5.22, 5.06 (d, d, $^3J = 10$ Hz, 1H, 1H, CHCH). ^{13}C NMR (100 MHz, CDCl_3 , TMS): δ 208.3, 207.6, 170.6 (C=S), 143.5 (C=N), 138.7, 135.5, 131.9, 130.0, 129.5, 129.3, 129.2, 129.0, 128.9, 128.8, 128.6, 128.5, 128.3, 128.2, 128.0, 127.7, 127.4, 126.4, 126.3, 90.3, 68.8, 68.2.

2.3. Syntheses of $\text{Fe}_2(\text{CO})_6(\mu\text{-}\kappa^2\text{S}:\kappa^2\text{N-PhC(S)=NNCH(4-CH}_3\text{C}_6\text{H}_4)\text{CH(4-CH}_3\text{C}_6\text{H}_4)\text{N(CH(4-CH}_3\text{C}_6\text{H}_4)\text{N=CSPH)} (3)$ and $\text{Fe}(\text{CO})_3(\kappa^2\text{S}:\text{N-PhC(=S)NHNCH(4-CH}_3\text{C}_6\text{H}_4)\text{CH(4-CH}_3\text{C}_6\text{H}_4)\text{N(CH(4-CH}_3\text{C}_6\text{H}_4)\text{N=CSPH)} (4)$

The same procedure was used, but 4- $\text{CH}_3\text{C}_6\text{H}_4\text{CH=NNHCSPH}$ (0.254 g, 1 mmol) was the added thioacylhydrazone. Elution with petroleum ether (60–90 °C) afforded red solids of **3** (0.116 g, Mp., 145–147 °C) and **4** (0.056 g, Mp., 105–106 °C) in yields of 26 and 15%. Anal. Calcd for $\text{C}_{44}\text{H}_{34}\text{Fe}_2\text{N}_4\text{O}_6\text{S}_2$ (**3**) (%): C, 59.34; H, 3.85; N, 6.29; found: C, 59.61; H, 3.94; N, 6.16. IR (KBr disk): 3079 (w), 3054 (w), 3031 (w), 2928 (w), 2924 (m), 2068 (vs), 1930 (vs), 1872 (m), 1586 (w), 1574 (w), 1270 (w), 1253 (w), 759 (m), 693 (m) cm^{-1} . ^1H NMR (600 MHz, CDCl_3 , TMS): δ 6.74–7.56 (m, 22H, $3\text{C}_6\text{H}_4$, $2\text{C}_6\text{H}_5$), 5.46 (s, 1H), 4.52, 4.25 (d, d, $^3J = 12$ Hz, 1H, 1H, CHCH), 2.42, 2.39, 2.36 (3s, 9H, 3CH_3). ^{13}C NMR (125 MHz, CDCl_3): δ 209.6, 208.6, 208.3, 161.6, 144.6, 138.3, 138.1, 137.85, 128.9, 128.7, 127.8, 127.3, 126.9, 126.8, 123.0, 121.4, 119.5, 84.2, 77.1, 69.0, 29.6, 26.8, 21.4. Anal. Calcd for $\text{C}_{41}\text{H}_{35}\text{FeN}_4\text{O}_3\text{S}_2$ (**4**) (%): C, 65.51; H, 4.69; N, 7.45; found: C, 65.56; H, 4.54; N, 7.52. IR (KBr disk): 3353 (w), 3035 (w), 2957 (w), 2924 (m), 2852 (w), 2066 (s), 2040 (s), 1995 (vs), 1698 (w), 1603 (s), 1499 (s), 1466 (w), 1375 (w), 1312 (w), 1277 (m), 1176 (m), 1024 (w), 995 (w), 959 (w), 879 (w), 822 (w), 753 (s), 691 (s) cm^{-1} . ^1H NMR (400 MHz, CDCl_3 , TMS): δ 6.62–7.97 (m, 22H, $3\text{C}_6\text{H}_4$, $2\text{C}_6\text{H}_5$), 5.83 (s, 1H), 5.72 (s, 1H), 5.11, 5.01 (d, d, $^3J = 10$ Hz, 1H, 1H, CHCH), 2.34, 2.22, 2.11 (3s, 9H, 3CH_3). ^{13}C NMR (100 MHz, CDCl_3 , TMS): δ 208.3, 207.6, 207.1, 170.2 (C=S), 143.2 (C=N), 138.7, 137.6, 137.1, 137.0, 136.4, 135.7, 132.6, 132.2, 132.0, 129.7, 129.2, 129.1, 128.8, 128.6, 128.4, 127.8, 127.4, 126.3, 126.1, 89.9, 68.2, 65.9, 29.6, 21.1, 21.0.

2.4. X-ray structure determinations of 1–4

Single crystals of **1–4** suitable for X-ray diffraction analyses were grown by slow evaporation of CH_2Cl_2 -petroleum ether solutions of **1–4** at 0–4 °C. For each of the complexes, a selected single crystal was mounted on a Bruker APEX2 CCD or Bruker D8quest CCD diffractometer which employed graphite-monochromated Mo- $\text{K}\alpha$ radiation ($\lambda = 0.71073$ Å) and data were collected at 296 K. The structures of **1–4** were solved by direct methods using the SIR-2011 software and refined by full-matrix least-squares based on F^2 with anisotropic thermal parameters for all non-hydrogen atoms using the SHELXTL package of programs [27, 28]. **1** and **4** are solvated by dichloromethane, with CH_2Cl_2 being disordered over two positions (63/37) (**1**) or located on an inversion center (**4**). For **3**, the phenyl group is disordered over two positions (73/27). All hydrogens in **1–4** were placed at geometrically idealized positions and subsequently treated as riding atoms, with C–H = 0.93 (aromatic), 0.98 (NCH), 0.97 (CH_2Cl_2) and 0.96 (CH_3) Å and U_{iso} (H) values of $1.2U_{\text{eq}}$ (C or N) or $1.5U_{\text{eq}}$ (C_{methyl}). Platon views of complexes are drawn using the PLATON software [29].

2.5. Electrochemical determinations of 1–4

Cyclic voltammetry experiments were carried out in a 5-mL one-compartment glass cell. The working electrode was a glassy carbon disk (0.3 cm in diameter), the reference electrode Ag⁺/Ag (0.01 M AgNO₃ in MeCN) and the counter electrode a Pt sheet. The electrolyte was 0.1 M ⁿBu₄NPF₆ in MeCN. The electrolyte solution was degassed by bubbling with N₂ for at least 10 min before measurement. The typical concentration of the organometallic complex was 1 mM. The acid concentration in the electrolyte was varied by addition of measured volumes of a solution of either HOTs (p-toluenesulfonic acid) or HOAc in MeCN.

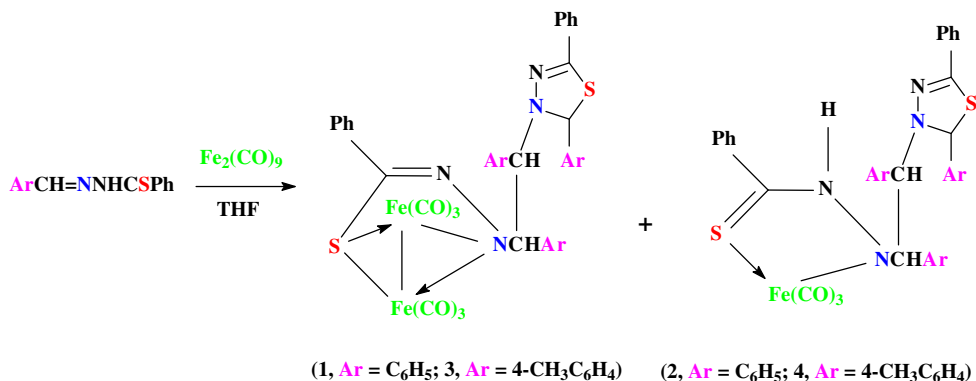
3. Results and discussion

3.1. Syntheses of 1–4

In view of a lack of investigations on the uses of thio-Schiff bases in organometallic chemistry [30, 31], the reactions of Fe₂(CO)₉ with thioacylhydrazones ArCH=NNHCSPh (Ar = C₆H₅, 4-CH₃C₆H₄) have been carried out. From the reactions, unexpected complexes Fe₂(CO)₆(μ-κ²S:κ²N-PhC(S)=NNR) (R = CHArCHArN(CHAr)N=CSPH; **1**, Ar = C₆H₅; **3**, Ar = 4-CH₃C₆H₄) and Fe(CO)₃(κ²S:N-PhC(=S)NHNr) (R = CHArCHArN(CHAr)N=CSPH; **2**, Ar = C₆H₅; **4**, Ar = 4-CH₃C₆H₄) have been obtained (scheme 1). TLC analyses show that using a 2 : 1 M ratio (Fe₂(CO)₉:ArCH=NNHCSPH) cleanly gives the respective products whereas using a 1 : 1 M ratio leads to excess thioacylhydrazones. To our knowledge, the two types of complexes with pendant bases are unprecedented despite the unclear mechanism of the above reactions [26].

3.2. X-ray structures of 1–4

Structures of the above complexes have been determined by X-ray crystallography. Details of crystal data, data collections, and structure refinements are presented in table 1. Selected geometric parameters are listed in table 2. As shown in figure 1, **1** contains a dianionic



Scheme 1. Syntheses of 1–4.

Table 1. Crystal data and structure refinements for 1–4.

	1	2	3	4
Formula	C ₄₁ H ₂₈ Fe ₂ N ₄ O ₆ S ₂ ·CH ₂ Cl ₂	C ₃₈ H ₂₀ FeN ₄ O ₃ S ₂	C ₄₄ H ₃₄ Fe ₂ N ₄ O ₆ S ₂	2(C ₄₁ H ₃₅ FeN ₄ O ₃ S ₂)·CH ₂ Cl ₂
<i>M_r</i>	933.42	709.62	890.57	1588.33
Cryst. system	Triclinic	Monoclinic	Monoclinic	Triclinic
Space group	<i>P</i> -1	<i>P</i> 2/ <i>n</i>	<i>P</i> 2 ₁ / <i>c</i>	<i>P</i> -1
<i>a</i> (Å)	10.5951(14)	9.1464(8)	11.3220(11)	9.442(2)
<i>b</i> (Å)	12.188(2)	12.2121(12)	10.2767(9)	9.8851(12)
<i>c</i> (Å)	18.4376(15)	31.025(3)	37.6317(15)	21.318(3)
<i>α</i> (°)	104.2366(15)	90.000	90.000	88.512(3)
<i>β</i> (°)	106.1904(12)	91.242(3)	96.2389(12)	79.915(3)
<i>γ</i> (°)	98.6430(19)	90.000	90.000	81.738(3)
<i>V</i> (Å ³)	2154.1(5)	3464.6(6)	4352.6(6)	1938.6(5)
<i>Z</i>	2	4	4	1
<i>D_c</i> (g cm ⁻³)	1.439	1.360	1.359	1.360
<i>μ</i> (mm ⁻¹)	0.945	0.599	0.813	0.609
<i>F</i> (0 0 0)	952	1468	1832	824
Reflections measured	19,471	33,733	37,292	27,305
Unique reflections	9937	7940	9991	8784
Reflections [<i>I</i> > 2σ(<i>I</i>)]	4209	5119	7373	5090
<i>R</i> _{int}	0.0591	0.0432	0.0345	0.0507
<i>θ</i> Range (°)	1.77–27.95	2.12–27.57	1.81–27.54	2.21–27.54
Data/restraints/parameters	9937/16/551	7940/0/433	9991/18/551	8784/0/481
Final <i>R</i> indices [<i>I</i> > 2.0σ(<i>I</i>)]	<i>R</i> ₁ , 0.0603; <i>wR</i> ₂ , 0.1360	<i>R</i> ₁ , 0.0588; <i>wR</i> ₂ , 0.1130	<i>R</i> ₁ , 0.0502; <i>wR</i> ₂ , 0.1102	<i>R</i> ₁ , 0.0564; <i>wR</i> ₂ , 0.1283
<i>R</i> indices (all data)	<i>R</i> ₁ , 0.1732; <i>wR</i> ₂ , 0.1867	<i>R</i> ₁ , 0.1083; <i>wR</i> ₂ , 0.1292	<i>R</i> ₁ , 0.0756; <i>wR</i> ₂ , 0.1215	<i>R</i> ₁ , 0.1198; <i>wR</i> ₂ , 0.1510
GOF	0.93	1.02	1.11	1.04
Max. peak and hole (e Å ⁻³)	0.776/−0.364	0.438/−0.457	0.386/−0.299	0.335/−0.486

Table 2. Selected geometric parameters (Å, °) for 1–4.

	1	2	3	4			
Fe1–Fe2	2.4078(11)	Fe1–S1	2.2009(8)	Fe1–Fe2	2.4005(6)	Fe1–S1	2.1855(10)
Fe1–S1	2.2878(14)	Fe1–N2	1.863(2)	Fe1–S1	2.2769(9)	Fe1–N2	1.876(2)
Fe2–S1	2.2801(14)	S1–C10	1.701(3)	Fe2–S1	2.2890(8)	S1–C10	1.700(3)
Fe1–N2	2.030(4)	S2–C31	1.771(3)	Fe1–N2	2.026(2)	S2–C33	1.763(3)
Fe2–N2	2.030(4)	S2–C32	1.812(3)	Fe2–N2	2.028(2)	S2–C34	1.833(3)
S1···N2	2.665(4)	N1–C10	1.305(3)	S1···N2	2.668(2)	N1–C10	1.314(3)
S1–C13	1.806(5)	N2–C11	1.492(3)	S1–C13	1.808(3)	N2–C11	1.486(3)
S2–C34	1.760(5)	N3–C18	1.468(3)	S2–C36	1.776(3)	N3–C19	1.474(3)
S2–C35	1.843(5)	N3–C32	1.474(3)	S2–C37	1.831(3)	N3–C34	1.460(3)
N1–C13	1.280(5)	N4–C31	1.274(3)	N1–C13	1.272(3)	N4–C33	1.280(3)
N2–C14	1.500(5)	N1–N2	1.331(3)	N2–C14	1.505(3)	N1–N2	1.329(3)
N3–C21	1.482(5)	N3–N4	1.391(3)	N3–C22	1.476(3)	N3–N4	1.394(3)
N3–C35	1.474(5)			N3–C37	1.480(3)		
N4–C34	1.296(5)			N4–C36	1.286(3)		
N1–N2	1.449(5)			N1–N2	1.438(3)		
N3–N4	1.400(5)			N3–N4	1.405(3)		
Fe1–S1–Fe2	63.62(4)	S1–Fe1–N2	83.64(7)	Fe1–S1–Fe2	63.44(2)	S1–Fe1–N2	83.82(7)
Fe1–N2–Fe2	72.76(12)	C1–Fe1–S1	174.34(12)	Fe1–N2–Fe2	72.60(7)	C1–Fe1–S1	169.07(13)

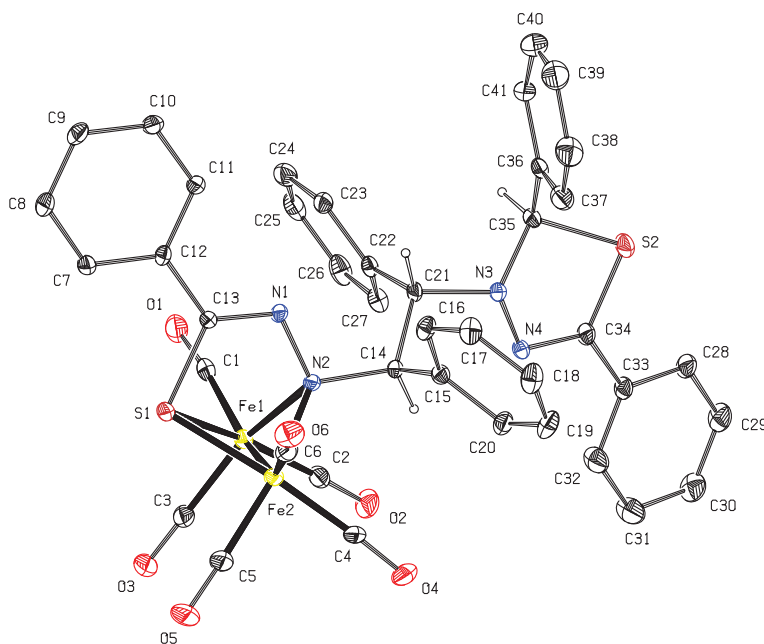


Figure 1. X-ray crystal structure of **1**, showing thermal ellipsoids at 20% probability.

ligand of the type $\text{PhC}(\text{S}^-)=\text{NNR}^-$ in which thiolato S and amido N each are four-electron donors. The S slightly asymmetrically bridges two $\text{Fe}(\text{CO})_3$ (I) units with 2.2878(14) and 2.2801(14) Å distances for Fe1–S1 and Fe2–S1, whereas the N symmetrically links the same units with equal bond distances of 2.030(4) (Fe1–N2) and 2.030(4) Å (Fe2–N2). The Fe1–S1–Fe2 and Fe1–N2–Fe2 bond angles are 63.62(4) and 72.76(12)°, and the dihedral angle between the Fe1S1Fe2 and Fe1N2Fe2 planes is 84.00(14)°. S1 is 0.0308(15) Å away from the C13N1N2 plane, indicating that the four-membered bridge is planar. The S1C13N1N2 plane makes dihedral angles of 89.8(2) and 89.8(2)° with these two planes, confirming that the S1C13N1N2 moiety of the ligand is perpendicular to the iron–iron axis. The S1C13N1N2 plane makes a dihedral angle of 2.8(3)° with the C7–C12–C11 plane. The iron centers are in a distorted octahedral environment, obeying the 18-electron rule. It can also be seen that the two tricarbonyl groups on Fe1 and Fe2 are eclipsed and all COs are terminal. The iron–iron bond distance is 2.4078(11) Å and markedly shorter than those of other nitrogen-bridged diiron complexes [30, 31]. The C13N1 and C34N4 bonds of 1.280(5) and 1.296(5) Å indicate that they are double bonds while the C13S1 bond of 1.806(5) Å is a single bond. Notably, the dihydrothiadiazole ring is not planar, the S1···N2 distance of 2.665(4) Å proves the presence of a strong intramolecular contact in **1** (R , van der Waals radius; $R(\text{S}) + R(\text{N}) = 3.35$ Å).

Complex **2**, shown in figure 2, is mononuclear (scheme 1). The five-coordinate Fe1 adopts a trigonal bipyramidal geometry, with S1 and N2 occupying axial and equatorial positions and S1–Fe1–N2 and S1–Fe1–C1 bond angles of 83.64(7) and 174.34(12)°. Three terminal CO ligands are not equivalent. The Fe1S1C10N1N2 five-membered ring is planar, with the Fe1 atom being 0.0427(4) Å away from the S1C10N1N2 plane. The S1C10N1N2 plane with the C4–C9–C8 plane forms a dihedral angle of 27.41(15)°. Unlike **1**, the C10S1

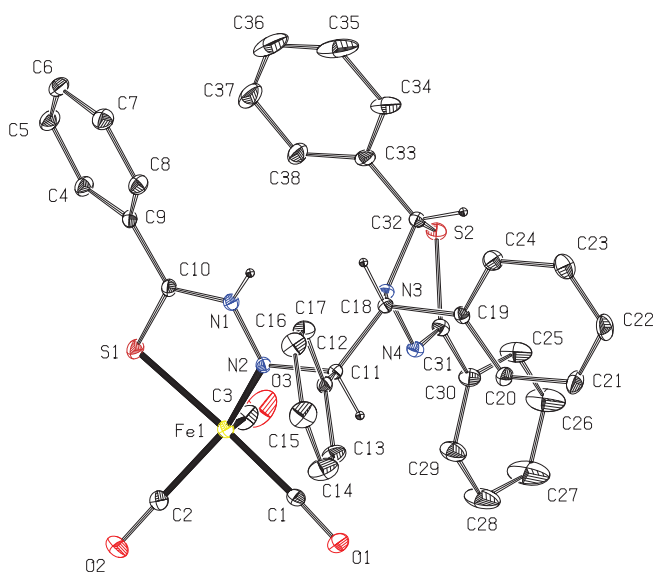


Figure 2. X-ray crystal structure of **2**, showing thermal ellipsoids at 20% probability.

bond of 1.701(3) Å is a double bond. The ligand PhC(=S)NHN^- is a monoanion, the Fe(CO)_3 unit is positively monovalent, and therefore, **2** is a 17-electron structure. The Fe–S and Fe–N bonds of 2.2009(8) and 1.863(2) Å are significantly shorter than those of **1**. Two Ar groups in **2** are cis, with the torsion angle of C12C11C18C19 in **2** being 59.8(3)° while the torsion angle of C15C14C21C22 in **1** is $-172.1(4)^\circ$.

As seen from figure 3, **3** has a dianionic ligand of type $\text{PhC(S}^-\text{)=NNR}^-$ similar to that in **1**, differing in the R group attached to the amido N (see above). Although the corresponding bond distances and angles in **3** are very similar to those in **1**, the most striking difference between them lies in configurations of the CHAr groups. Unlike **1**, two Ar groups in **3** are cis, with the torsion angle of C15C14C22C23 in **3** of 54.7(2)°. The C30–C35 Ar ring is two-site disordered ($\sim 3 : 1$) and only the major component is shown in figure 3 similar to **1**, S slightly asymmetrically links the two Fe(CO)_3 (I) fragments with 2.2769(9) and 2.2890(8) Å bond distances for Fe1–S1 and Fe2–S1, whereas N symmetrically bridges the same fragments with bond distances of 2.026(2) (Fe1–N2) and 2.028(2) Å (Fe2–N2). The Fe1–S1–Fe2 and Fe1–N2–Fe2 bond angles are 63.44(2) and 72.60(7)° while the dihedral angle between the Fe1S1Fe2 and Fe1N2Fe2 planes is 83.86(7)°. S1 is 0.0122(8) Å away from the C13N1N2 plane, showing that the four atoms bridging the two irons are coplanar. The S1C13N1N2 plane makes dihedral angles of 88.54(10) and 89.04(12)° with respect to those planes, confirming that S1C13N1N2 of the ligand is almost perpendicular to the iron–iron axis. The S1C13N1N2 plane forms a dihedral angle of 30.95(15)° with the C7–C12–C11 plane. The iron centers are again in a distorted octahedral environment, satisfying the 18-electron rule. The two tricarbonyl groups on Fe1 and Fe2 are eclipsed and all COs are terminal. The iron–iron distance of 2.4005(6) Å is very close to that of **1**. To our knowledge, this is the shortest Fe–Fe bond among reported complexes with N donors [30, 31]. The bond distances of 1.272(3) Å for C13N1, 1.286(3) Å for C36N4, and 1.808(3) Å for C13S1 may be compared with those of **1**. As noted in **1**, the five-membered heterocycle of

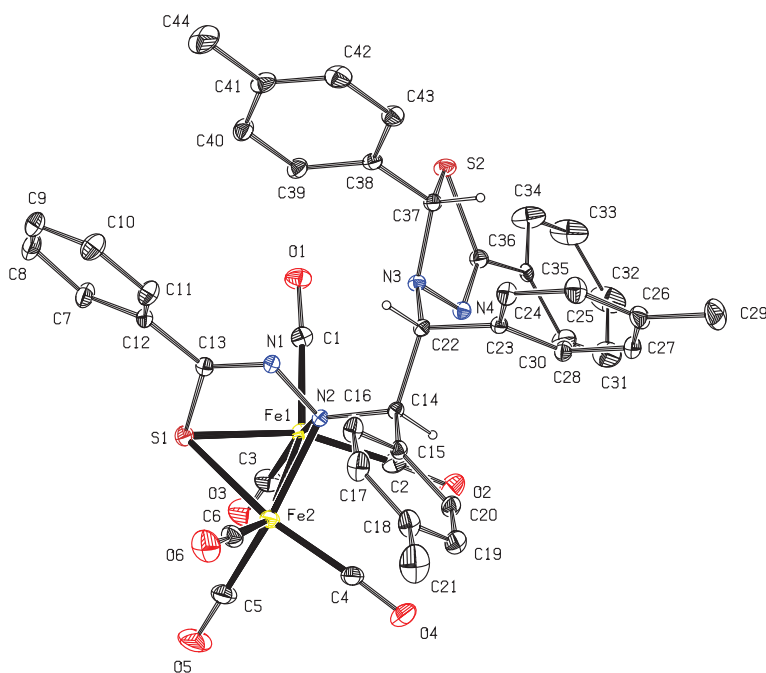


Figure 3. X-ray crystal structure of **3**, showing thermal ellipsoids at 20% probability.

C37N3N4C36S2 is puckered with the S1···N2 distance of 2.668(2) Å, indicating that a strong intramolecular contact exists in **3**.

Complex **4**, displayed in figure 4, is mononuclear and has a similar monoanionic ligand of type PhC(=S)NHNR⁻ to that in **2**, differing in the R group attached to the amido N (scheme 1). The five-coordinate Fe1 possesses a trigonal bipyramidal geometry, with S1 and N2 occupying axial and equatorial positions and S1–Fe1–N2 and S1–Fe1–C1 bond angles of 83.82(7) and 169.07(13)°. The three terminal CO ligands are not equivalent. The Fe1S1C10N1N2 five-membered ring is not planar, with Fe1 being 0.1491(4) Å away from the S1C10N1N2 plane. The S1C10N1N2 plane forms a dihedral angle of 4.2(3)° with the C4–C9–C8 plane. As in **2**, the C10S1 bond of 1.700(3) Å is a double bond. The ligand PhC(=S)NHNR⁻ functions as a monoanion, the Fe(CO)₃ unit is positively monovalent, and thus, **4** is a 17-electron species. If the ligand were PhC(S⁻)=NNR⁻, **4** as well as **2** would be 16-electron. The Fe–S and Fe–N bonds of 2.1855(10) and 1.876(2) Å are clearly shorter than those of **1** and **3**, but closer to those of **2**. Unlike **2** and **3**, the two Ar groups in **4** are trans, with the C12C11C19C20 torsion angle being 179.6(2)°.

3.3. Spectroscopic characteristics of 1–4

The complexes have also been characterized by IR, ¹H NMR, and ¹³C NMR spectroscopies (see the Supplemental data). In the IR spectrum of **1**, the terminal carbonyl groups show four absorptions at 1983–2074 cm⁻¹. For **3**, the terminal carbonyl groups are three peaks at 1872–2068 cm⁻¹. In the IR spectra of **2** and **4**, the terminal carbonyl groups show three

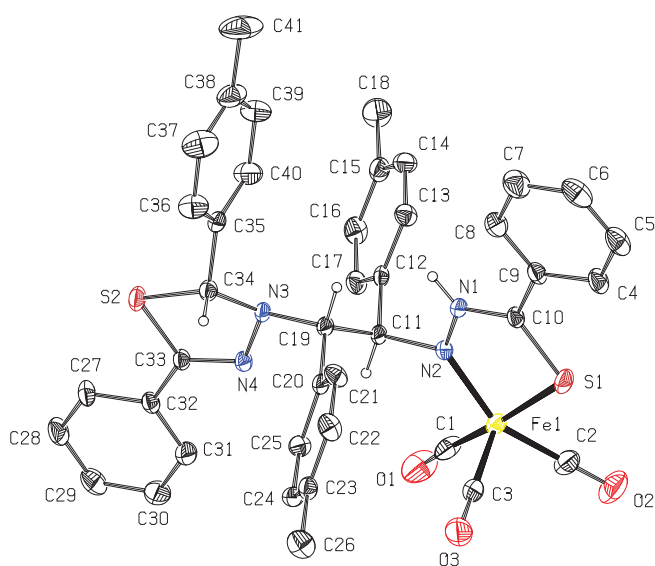


Figure 4. X-ray crystal structure of **4**, showing thermal ellipsoids at 20% probability.

absorptions from 1996 to 2067 and 1995–2066 cm^{-1} . In particular, the N–H vibration appears at 3348 for **2** and 3353 cm^{-1} for **4**.

In the ^1H NMR spectra of **1** and **3**, the NCHARCHARN group shows two AB-type doublets at 4.58 and 4.32 ppm for **1** with $^3J = 12$ Hz and 4.52 and 4.25 ppm for **3** with $^3J = 12$ Hz. The NCHARS group occurs as a singlet at 5.44 ppm for **1** and 5.46 ppm for **3**. All the Ar groups are multiplets at 7.59–6.86 ppm for **1** and 7.56–6.74 ppm for **3**. The three methyl groups in **3** display three singlets at 2.42, 2.39, and 2.36 ppm. In the ^{13}C NMR spectrum of **1**, the terminal CO groups are five singlets from 214.5 to 203.2 ppm whereas

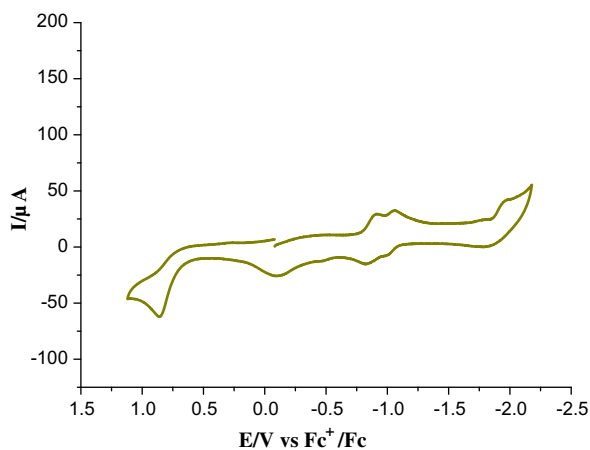


Figure 5. Cyclic voltammogram of **1** (1.0 mM) in 0.1 M $n\text{Bu}_4\text{NPF}_6/\text{MeCN}$ at a scan rate of 100 mV s^{-1} .

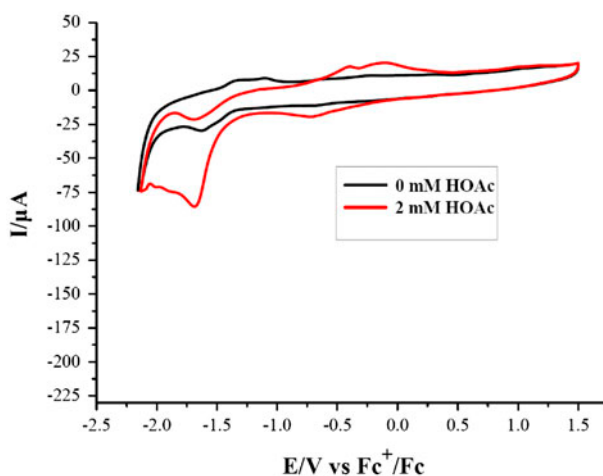


Figure 6. Cyclic voltammograms of **2** (1.0 mM) with HOAc in 0.1 M ⁿBu₄NPF₆/MeCN at a scan rate of 100 mV s⁻¹.

those of **3** exhibit three singlets at 209.6–208.3 ppm in agreement with literature values [17–22]. The two C=N groups display two singlets at 163.3, 147.1 ppm for **1** and at 161.6, 144.6 ppm for **3**. Except for Ar signals, all the CH groups as well as the CH₃ groups for **3** show anticipated resonances. In the ¹H NMR spectra of **2** and **4**, the NCHArCHARN group shows two doublets at 5.22 and 5.06 ppm for **2** with ³J = 10 Hz and 5.11 and 5.01 ppm for **4** with ³J = 10 Hz. The NH and NCHArS groups occur as two singlets at 5.85 and 5.76 ppm for **2** and 5.83 and 5.72 ppm for **4**. D₂O exchange experiments did not afford positive information on the NH and NCHArS groups; neither of the two singlets disappeared. All the Ar groups occur as multiplets from 7.97 to 6.96 ppm for **2** and 7.97–6.62 ppm for **4**. The three methyl groups in **4** display three singlets at 2.34, 2.22, and 2.11 ppm. In the ¹³C NMR spectrum of **2**, the terminal CO groups appear as singlets at 207.6 and 208.3 ppm whereas those of **4** exhibit three singlets at 207.1, 207.6, and 208.3 ppm. The C=S group displays one singlet at 170.6 ppm for **2** and at 170.2 ppm for **4**. All the CH groups as well as the CH₃ groups for **4** show the expected resonances. As such, except for the CO signals in solution, the spectroscopic data are in agreement with their crystal structures [17–22].

3.4. Electrochemistry of 1–4

To obtain an estimate of their capability to catalyze hydrogen production, cyclic voltammetry (CV) of **1–4** (figures 5–8) has been performed (table 1S). The reductive peaks from -1.95 to -1.98 V and -1.004 to -1.005 V are ascribed to the one-electron process Fe(I)Fe(0)/Fe(0)Fe(0) and Fe(I)Fe(I)/Fe(I)Fe(0) and the oxidation peaks at 0.83–0.85 V are assigned to the Fe(I)Fe(I)/Fe(II)Fe(I) process, whereas the other peaks observed are due to the ligand [5, 32–37]. The catalytic proton reduction by **1** and **3** was studied through cyclic voltammetry upon addition of HOTs (pK_a ≈ 8) in CH₃CN, with the concentration of 0–10 mM. Unfortunately, their redox behaviors are too complex to be explained at this point, due to the presence of three proton donors. However, using HOAc (pK_a ≈ 23, in

CH₃CN) as a proton source does not lead to the above cases. As shown in figure 7, **3** shows high catalytic efficiency ($CE = (i_{cat}/i_d)/(C_{HA}/C_{cat})$, where i_{cat} is the catalytic current, i_d is the current for reduction of the catalyst in the absence of acid, C_{HA} is the acid concentration, and C_{cat} is the catalyst concentration [5]) at the reduction peak of -1.98 V ($CE = 0.91$), with increasing amount of the acid, the reduction current increases [36, 37]. In other words, H₂ is catalytically produced by 3^{2-} . Catalytic proton reduction by **2** and **4** was also investigated via cyclic voltammetry on addition of HOAc in CH₃CN. Complexes **2** and **4** exhibit catalytic behavior at the reduction peak of -1.62 V ($CE = 0.95$) for **2** and -1.92 V ($CE = 0.81$) for **4**.

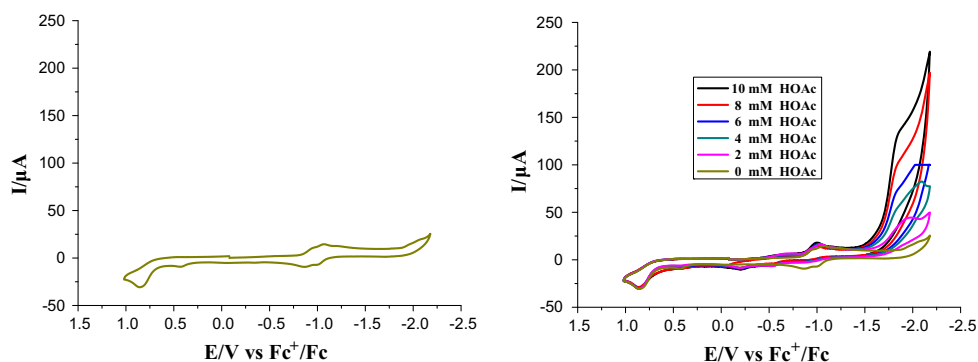


Figure 7. Cyclic voltammograms of **3** (1.0 mM) with HOAc (0–10 mM) in 0.1 M ^tBu₄NPF₆/MeCN at a scan rate of 100 mV s⁻¹ (left, without HOAc; right, 0–10 mM HOAc).

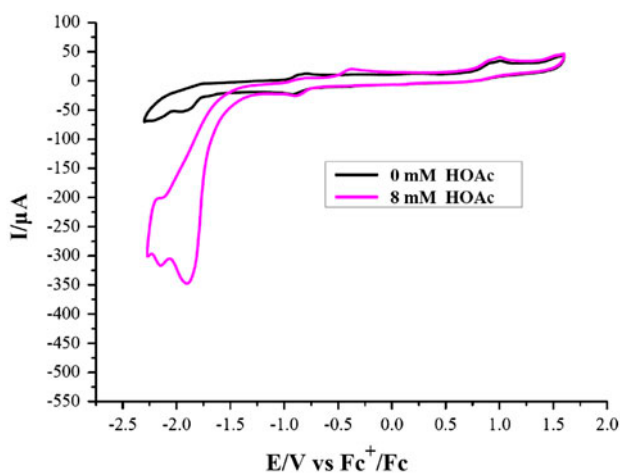


Figure 8. Cyclic voltammograms of **4** (1.0 mM) with HOAc in 0.1 M ^tBu₄NPF₆/MeCN at a scan rate of 100 mV s⁻¹.

4. Conclusion

Reactions of Fe₂(CO)₉ with thioacylhydrazones afford Fe₂(CO)₆(μ-κ²S:κ²N-PhC(S)=NNR) and Fe(CO)₃(μ-κ²S:κ²N-PhC(=S)NHNHNR). Their structures have been determined by X-ray crystallography. Electrochemical studies confirm that they show catalytic H₂-producing activity in the presence of proton donors. Reactions of thiosemicarbazones with iron carbonyls are under investigation.

Supplementary material

CCDC 983053 (1), 1043668 (2), 983054 (3) and 1043669 (4) contain the supplementary crystallographic data (including structure factors) for this paper. These data can be obtained free of charge from the Cambridge Crystallographic Data Centre via www.ccdc.cam.ac.uk/data_request/cif.

Disclosure statement

The authors declare no competing financial interest.

Funding

This work was supported by the Mao Zedong Foundation of China; Project Funded by the Priority Academic Program Development of Jiangsu Higher Education Institutions (PAPD); Natural Science Foundation of China [grant number 20572091]; Natural Science Foundation of Jiangsu Province [grant number 05KJB150151].

Supplemental data

Supplementary data including IR, NMR and CV data for this article can be accessed at <http://dx.doi.org/10.1080/00958972.2015.1062479>.

References

- [1] T.R. Simmons, G. Berggren, M. Bacchi, M. Fontecave, V. Artero. *Coord. Chem. Rev.*, **270–271**, 127 (2014).
- [2] J.-F. Capon, F. Gloaguen, F.Y. Pétilon, P. Schollhammer, J. Talarmin. *Coord. Chem. Rev.*, **253**, 1476 (2009).
- [3] C. Tard, C.J. Pickett. *Chem. Rev.*, **109**, 2245 (2009).
- [4] F. Gloaguen, T.B. Rauchfuss. *Chem. Soc. Rev.*, **38**, 100 (2009).
- [5] G.A.N. Felton, C.A. Mebi, B.J. Petro, A.K. Vannucci, D.H. Evans, R.S. Glass, D.L. Lichtenberger. *J. Organomet. Chem.*, **694**, 2681 (2009).
- [6] D.M. Heinekey. *J. Organomet. Chem.*, **694**, 2671 (2009).
- [7] S. Ogo, R. Kabe, K. Uehara, B. Kure, T. Nishimura, S.C. Menon, R. Harada, S. Fukuzumi, Y. Higuchi, T. Ohhara, T. Tamada, R. Kuroki. *Science*, **316**, 585 (2007).
- [8] A.D. Wilson, R.K. Shoemaker, A. Miedaner, J.T. Muckerman, D.L. DuBois, M.R. DuBois. *Proc. Natl. Acad. Sci. USA*, **104**, 6951 (2007).
- [9] Y. Ohki, K. Yasumura, K. Kuge, S. Tanino, M. Ando, Z. Li, K. Tatsumi. *Proc. Natl. Acad. Sci. USA*, **105**, 7652 (2008).
- [10] L.-C. Song, M.-Y. Tang, F.-H. Su, Q.-M. Hu. *Angew. Chem. Int. Ed.*, **45**, 1130 (2006).
- [11] L.-C. Song, L.-X. Wang, M.-Y. Tang, C.-G. Li, H.-B. Song, Q.-M. Hu. *Organometallics*, **28**, 3834 (2009).
- [12] M.Y. Darensbourg, E.J. Lyon, X. Zhao, I.P. Georgakaki. *Proc. Natl. Acad. Sci. USA*, **100**, 3683 (2003).
- [13] M.L. Singleton, N. Bhuvanesh, J.H. Reibenspies, M.Y. Darensbourg. *Angew. Chem. Int. Ed.*, **47**, 9492 (2008).
- [14] (a) Ö.F. Erdem, L. Schwartz, M. Stein, A. Silakov, S. Kaur-Ghumaan, P. Huang, S. Ott, E.J. Reijerse, W. Lubitz. *Angew. Chem. Int. Ed.*, **50**, 1439 (2011); (b) M. Karnahl, A. Orthaber, S. Tschierlei, L. Nagarajan, S. Ott. *J. Coord. Chem.*, **65**, 2713 (2012).

- [15] (a) Y.-C. Liu, K.-T. Chu, R.-L. Jhang, G.-H. Lee, M.-H. Chiang. *Chem. Commun.*, **49**, 4743 (2013); (b) F. Quentel, G. Passard, F. Gloaguen. *Energy Environ. Sci.*, **5**, 7757 (2012).
- [16] P.-Y. Orain, J.-F. Capon, F. Gloaguen, F.Y. Pétillon, P. Schollhammer, J. Talarmin, G. Zampella, L. De Gioia, T. Roisnel. *Inorg. Chem.*, **49**, 5003 (2010).
- [17] Y.-C. Shi, H. Tan, Y. Shi. *Polyhedron*, **67**, 218 (2014).
- [18] W. Yang, Q. Fu, J. Zhao, H.-R. Cheng, Y.-C. Shi. *Acta Crystallogr., Sect. C*, **70**, 528 (2014).
- [19] Y.-C. Shi, W. Yang, Y. Shi, D.-C. Cheng. *J. Coord. Chem.*, **67**, 2330 (2014).
- [20] Y.-C. Shi, F. Gu. *Chem. Commun.*, **49**, 2255 (2013).
- [21] (a) Y.-C. Shi, H.-R. Cheng, Q. Fu, F. Gu, Y.-H. Wu. *Polyhedron*, **56**, 160 (2013); (b) Y.-C. Shi, Q. Fu. *Z. Anorg. Allg. Chem.*, **639**, 1791 (2013); (c) Y.-C. Shi, H.-R. Cheng, D.-C. Cheng. *Acta Crystallogr., Sect. C*, **69**, 581 (2013).
- [22] (a) Y.-C. Shi, H.-R. Cheng, H. Tan. *J. Organomet. Chem.*, **716**, 39 (2012); (b) Y.-C. Shi, H.-R. Cheng, L.-M. Yuan, Q.-K. Li. *Acta Crystallogr.*, **E67**, m1534 (2011).
- [23] Y.-C. Shi, Y. Shi, W. Yang. *J. Organomet. Chem.*, **772–773**, 131 (2014).
- [24] Y.-C. Shi, H.-M. Yang, H.-B. Song, C.-G. Yan, X.-Y. Hu. *Polyhedron*, **23**, 567 (2004).
- [25] Y.-C. Shi. *J. Coord. Chem.*, **57**, 961 (2004).
- [26] D.S. Kalinowski, P.C. Sharpe, P.V. Bernhardt, D.R. Richardson. *J. Med. Chem.*, **50**, 6212 (2007).
- [27] M.C. Burla, R. Caliendo, M. Camalli, B. Carrozzini, G.L. Cascarano, C. Giacovazzo, M. Mallamo, A. Mazzone, G. Polidori, R. Spagna. *J. Appl. Crystallogr.*, **45**, 357 (2012).
- [28] G.M. Sheldrick. *Acta Crystallogr.*, **A64**, 112 (2008).
- [29] (a) L.J. Farrugia. *J. Appl. Crystallogr.*, **45**, 849 (2012); (b) A.L. Spek. *Acta Crystallogr.*, **D65**, 148 (2009).
- [30] C.-Y. Wu, L.-H. Chen, W.-S. Hwang, H.-S. Chen, C.-H. Hung. *J. Organomet. Chem.*, **689**, 2192 (2004).
- [31] W. Imhof, A. Göbel, L. Schweda, D. Dönnecke, K. Halbauer. *J. Organomet. Chem.*, **690**, 3886 (2005).
- [32] Z. Wang, W.-F. Jiang, J.-H. Liu, W.-N. Jiang, Y. Wang, B. Åkermark, L.-C. Sun. *J. Organomet. Chem.*, **693**, 2828 (2008).
- [33] J.-F. Capon, F. Gloaguen, P. Schollhammer, J. Talarmin. *J. Electroanal. Chem.*, **595**, 47 (2006).
- [34] S. Ezzaher, J.-F. Capon, F. Gloaguen, F.Y. Pétillon, P. Schollhammer, J. Talarmin, N. Kervarec. *Inorg. Chem.*, **48**, 2 (2009).
- [35] P.-H. Zhao, K.-K. Xiong, W.-J. Liang, E.-J. Hao. *J. Coord. Chem.*, **68**, 968 (2015).
- [36] F. Gloaguen, J.D. Lawrence, T.B. Rauchfuss. *J. Am. Chem. Soc.*, **123**, 9476 (2001).
- [37] L.-C. Song, C.-G. Li, J. Gao, B.-S. Yin, X. Luo, X.-G. Zhang, H.-L. Bao, Q.-M. Hu. *Inorg. Chem.*, **47**, 4545 (2008).